Supplementary Information (SI)

Photo, pH and redox multi-responsive nanogels for drug delivery and fluorescence cell imaging

Shuo Chen,[a,b] Qing Bian,[a] Panjun Wang,[a] Xuewei Zheng,[a] Le Lv, [c,*] Zhimin Dang [b,*] and Guojie Wang[a,*]

[a]School of Materials Science and Engineering, University of Science and Technology Beijing, Beijing 100083, China

*E-mail: guojie.wang@mater.ustb.edu.cn; Tel: 86-10-62333619;

[b] Department of Polymer Science and Engineering, University of Science and Technology Beijing, Beijing 100083, China

*E-mail: dangzm@ustb.edu.cn; Tel: 86-10-62332599;

[c] Department of Biological Science and Engineering, University of Science and Technology Beijing, Beijing 100083, China

*E-mail: lvle@ustb.edu.cn; Tel: 86-10-62334497.

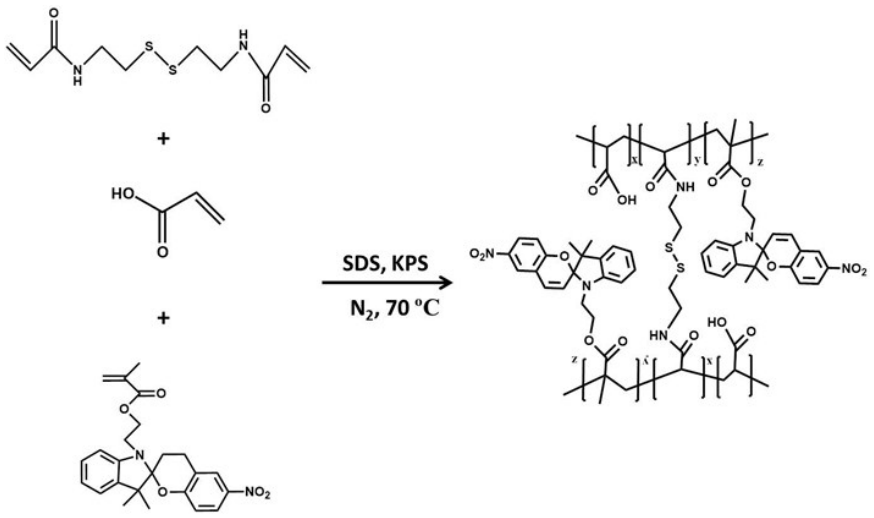

Figure S1. Synthetic route of SP-based nanogels.

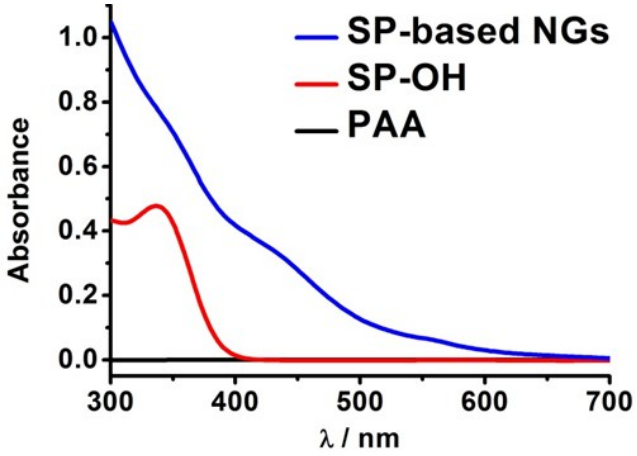

Figure S2. UV-vis absorption spectra of SP-based NGs aqueous solution (1 mg mL^{-1}), SP-OH in THF (0.028 mg mL^{-1}) and PAA aqueous solution (1.5 mg mL^{-1}).

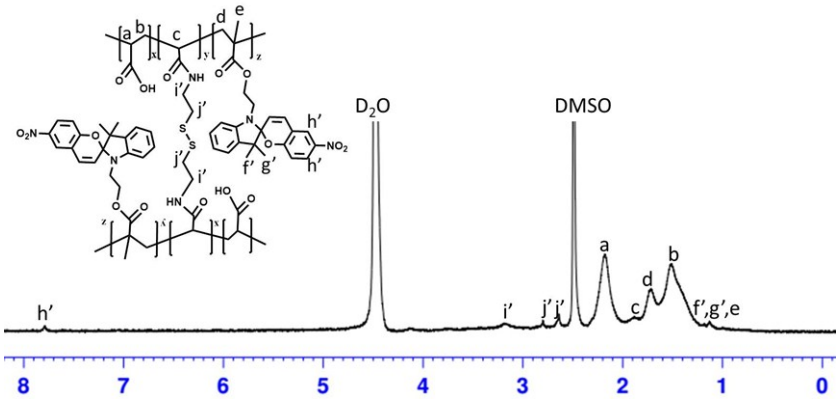

Figure S3. ^{1}H NMR spectrum of SP-based nanogels in D_2O and deuterated DMSO (V_{D_2O}:$V_{\text{deuterated DMSO}}$=1:10).

The functionalization degree of SP on the NGs was calculated to be 3.53% by comparing the integral values of the band centered at 7.82 ppm (ortho hydrogen of nitrobenzene in SP) and the band centered at 2.23 ppm (methine group in PAA), shown in Figure S3. The functionalization degree of SP on the NGs determined by ^{1}H NMR was lower than that determined by UV-vis absorption spectrum due to encapsulation effects of SP.

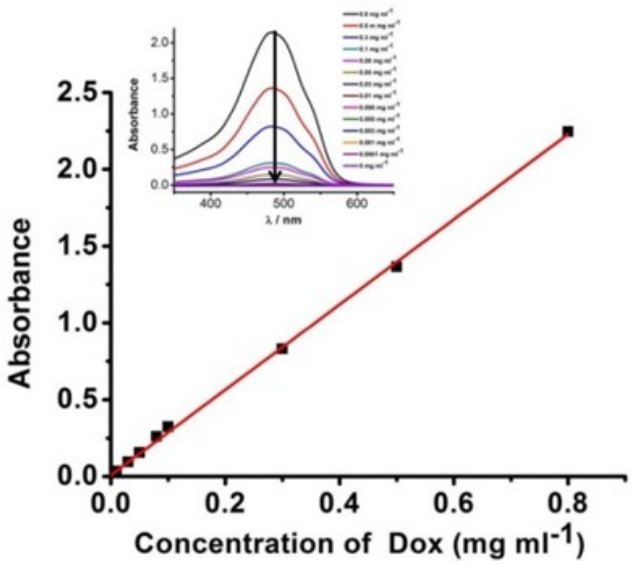

Figure S4. Calibrated curve of Dox·HCl concentration. Inset: UV-vis absorption spectra of Dox·HCl solution with different concentrations.

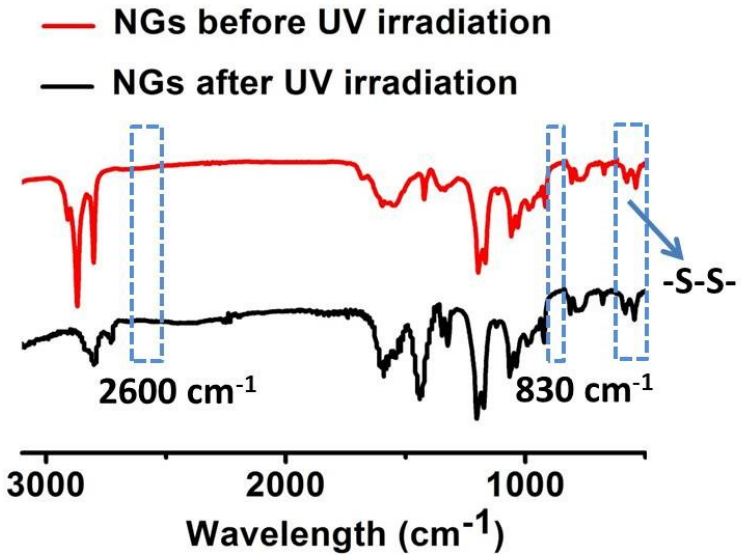

Figure S5. FT-IR spectra of NGs before and after UV light irradiation.

The FT-IR spectra of NGs before and after UV light irradiation are shown in Fig. S5, from which it can be seen that most characteristic peaks of the NGs after UV light irradiation were overlaid by the characteristic absorption of NGs before UV light irradiation. The strong absorption bands centered at 520-560 cm^{-1} of SP-based NGs were ascribed to disulfide bridges.[s1] If the photo-induced cleavage of disulfides happened after UV irradiation,[s2] mercapto groups (S-H) and sulfonic acid groups (SO_3H) would be formed, then the S-H stretching absorption band centered at 2600 cm^{-1} and S-OH stretching absorption band centered at 830 cm^{-1} would appear in the spectrum.[s3,s4] However, there are no absorption bands centered at 2600 cm^{-1} and 830 cm^{-1} in the FT-IR spectrum of NGs after UV irradiation. The results confirm that the disulfides of NGs could not be cleaved after short time UV light irradiation with low-intensity lamps in this work.

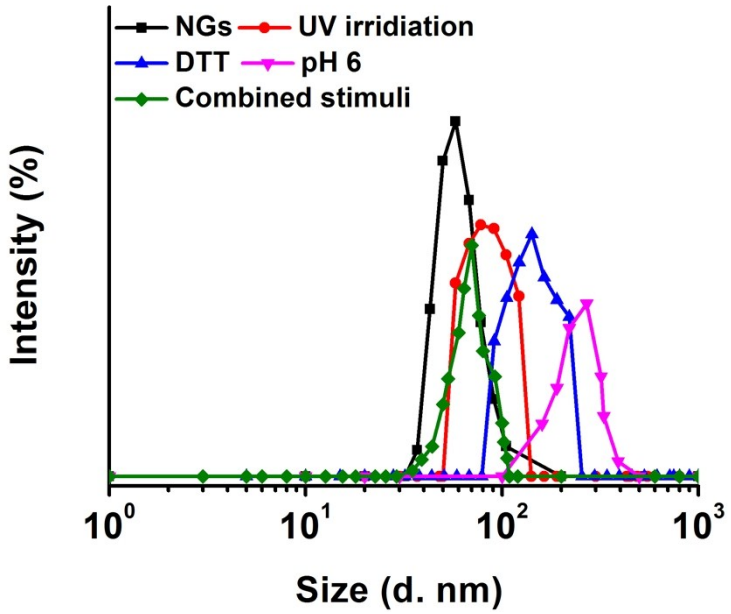

Figure S6. Intensity-based size distributions of the SP-based NGs under different stimuli: (a) NGs without stimulation (b) after UV irradiation for 1 min; (c) at pH 6 for 12 h; (d) in the presence of DTT (4 mM) for 12 h; (e) combined stimulation of UV light irradiation (1 min), pH 6 and in the presence of DTT (4 mM) for 12 h.

Fig. S6 shows the intensity-based size distribution of the SP-based NGs in water before and after the stimulation. The sizes of the primary NGs, NGs after UV irradiation, NGs at pH 6, NGs in the presence of DTT and NGs under combined stimulation of UV irradiation, pH6 and DTT determined by intensity based DLS were 72 nm, 94 nm, 269 nm, 162 nm and 53 nm respectively, which were consistent with those determined by number based DLS.

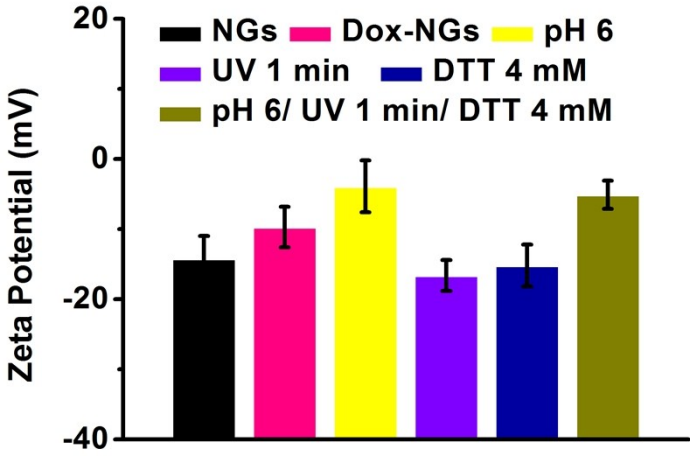

Figure S7. Zeta potentials of NGs, NGs under different stimulation and Dox-loaded NGs.

Fig. S7 shows the surface zeta potentials of primary NGs, NGs under different stimulation and Dox-loaded NGs. The surface zeta potential of primary NGs in water was -14.6 mV. The surface zeta potentials of NGs under UV light irradiation and in the presence of DTT were measured to be -16.3 mV and -15.8 mV respectively, which were similar to that of primary NGs. At pH 6, the surface zeta potential of NGs increased to -5.3 mV, since more carboxyl groups on NGs were protonated at lower pH value. Under combined stimulation of pH 6, UV light and DTT, the surface zeta potential of NGs was about -7.2 mV. Compared with the surface zeta potential of primary NGs, the surface zeta potential of Dox-loaded NGs increased to -9.8 mV, since the drug doxorubicin hydrochloride was positively charged.

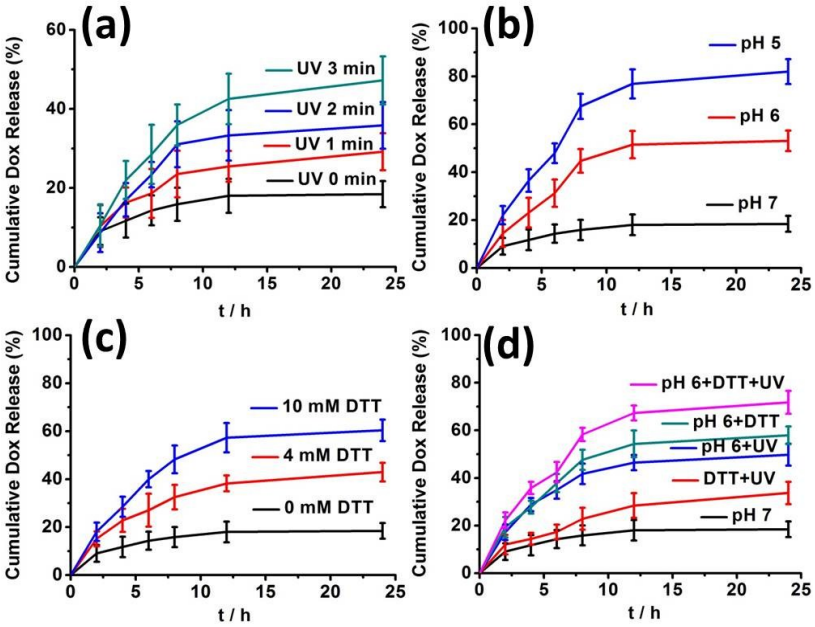

Figure S8. Release profiles of Dox loaded in the SP-based NGs under different stimulation in saline condition: a) after UV light irradiation for different time at pH 7 and kept for 24 h; b) at different pH values for 24 h; c) in the presence of DTT with different concentrations at pH 7 for 24 h; d) under different combined stimulation.

Fig. S8a shows the release profiles under the saline condition with UV light irradiation. When the irradiation time increased from 0 to 1, 2, and 3 min, the cumulative release in 24 h increased from 17% to 26%, 35% and 49%, respectively. Fig. S8b shows the release profiles under the saline condition at different pH values for 24 h. At pH 7, only about 15% of the loaded Dox was released from the NGs in 24 h. At pH 6, 46% of the loaded Dox was released in 24 h, while 82% of the loaded Dox was released at pH 5. Fig. S8c shows the release profiles under the saline condition at different DTT concentrations. When the DTT concentration increased from 4 mM to 10 mM, the cumulative release in 24 h increased from 42% to 62%. Fig. S8d shows release profiles under the saline condition with different combined stimuli. Under dual stimulation of DTT 4 mM and UV irradiation 1 min, pH 6 and UV irradiation 1 min, and pH 6 and DTT 4 mM, the cumulative release in 24 h was about 31%, 44% and 53% respectively. The cumulative release under combined stimulation was

higher than that under corresponding single stimulation. Under triple stimulation of UV light, pH 6 and DTT, the release amount of Dox dramatically increased to 72% in 24 h.

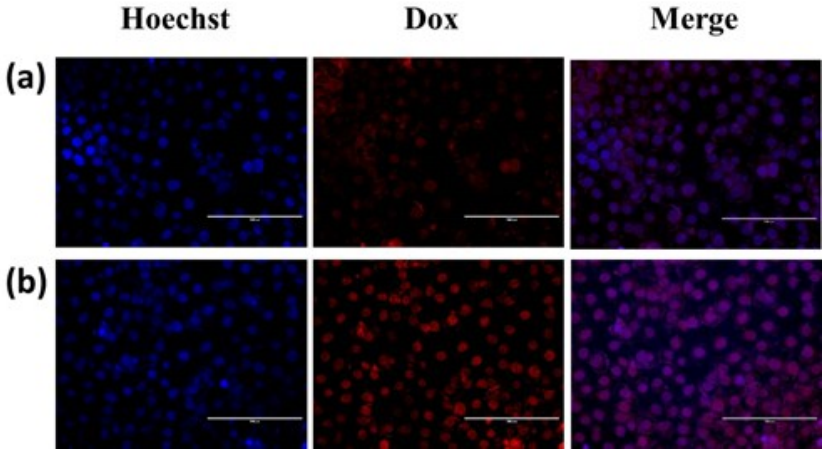

Figure S9. Fluorescence microscope observations of the Dox release in MFC-7 cells treated with Dox·HCl incubated for 2 h (a) and 4h (b). Scale bar 200 μm. For each panel, the images from left to right show cell nuclei stained by Hoechst (blue; Hoechst 33342), Dox fluorescence in cells (red) and overlays of the images.

Figure S9 shows the fluorescence images of MCF-7 cells incubated with Dox·HCL for different time. The fluorescence of MCF-7 cells incubated with Dox·HCL was similar with that of MCF-7 cancer cells incubated with Dox-loaded NGs after UV light irradiation (Fig. 6). This result indicated that Dox-loaded NGs could efficiently deliver the loaded anti-cancer Dox into the cancer cells.

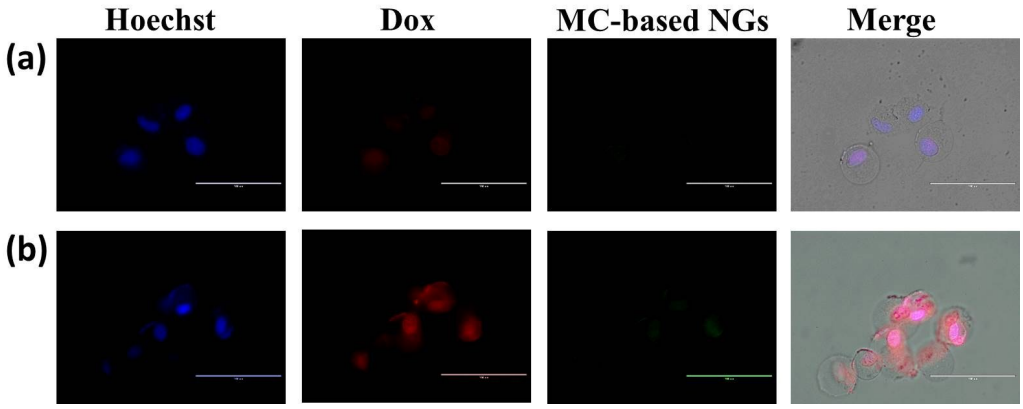

Figure S10. Fluorescence microscope images of the Dox and MC-based NGs in MCF-7 cells without UV light irradiation. a) MCF-7 cells treated with Dox-loaded NGs incubated for 2 h, b) MCF-7 cells treated with Dox-loaded NGs incubated for 4 h. Scale bar 100 µm. For each panel, the images from left to right show cells nuclei stained by Hoechst (blue; Hoechst 33342), Dox fluorescence in cells (red), MC-based NGs fluorescence in cells (green) and overlays of the three images.

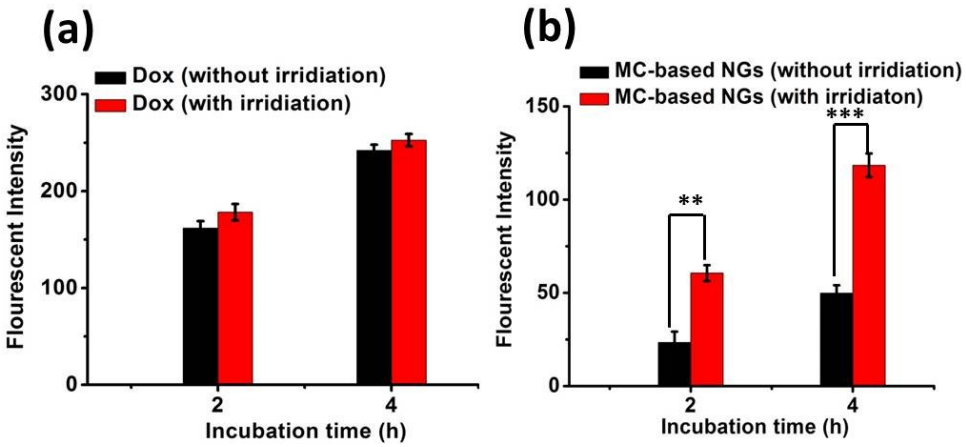

Figure S11. (a) Fluorescence intensities of Dox at different incubation time in MCF-7 cells. MCF-7 cells treated with Dox-loaded NGs with or without UV light irradiation for different incubated time. (b) Fluorescence intensities of MC-based NGs at different incubation time in MCF-7 cells. MCF-7 cells treated with NGs with or without UV light irradiation for different incubated time. Each set of data was represented as mean ± SD (n = 3, **p < 0.01, ***P < 0.001).

References

S1. N. N. Brandt, A. Y. Chikishev, A. A. Mankova and I. K. Sakodynskaya, *J. Biomed. Opt.,* 2015, **20**, 051015 (1-6).

S2. L. Y. Li, C. F. Song, M. Jennings and S. Thayumanavan, *Chem. Commun.,* 2015, **51**, 1425-1428.

S3. V. Krishnakumar and R. J. Xavier, *Spectrochim. Acta A*, 2004, **60**, 709-714.

S4. S. M. Chackalackal and F. E. Stafford, *J. Am. Chem. Soc.,* 1966, **88**, 4815-4819.